Thermodynamic Simulation of a Hybrid Thermo-Solar Externally Fired Gas Turbine Power Plant Fueled with Biomass.

Agustín Ghazarian[2], Daiana De León[2], Pedro Galione[2,b)], Pedro Curto[2], Alejandro Medina[1,a)], Antonio Calvo[1].

[1] Professor. Department of Applied Physics, University of Salamanca, Salamanca, Spain
+ 34 677565486.
[2] Departamento de Termodinámica Aplicada, Universidad de la República, Montevideo, Uruguay.

[a)]Corresponding author: amd385@usal.es
[b)]pgalione@fing.edu.uy

Abstract. A thermodynamic model for a hybrid thermo-solar externally fired gas turbine power plant fueled with biomass is presented. This technology represents a fully renewable way of obtaining electric power relying mainly in biomass with an extra advantage of decreasing its consumption at good radiative conditions. A concentrated solar power plant is implemented considering the Solugas project situated in Abengoa's Solúcar Platform near Seville. To predict its behavior two models were implemented and compared with experimental data presented in previous papers. Yearly evolution of the output power, fuel mass flow, overall efficiency and fuel conversion efficiency for a typical Uruguayan year is presented. In addition, global results are presented leading to a 1.5% fuel saving increasing the economic efficiency a 0.3% what denotes the solar field and tower cavity seem to be undersized.

INTRODUCTION.

Sustainable development of countries relies, among other factors, on the production of energy with reduced greenhouse gases emissions and conserving soil and water. Thus, future energy world supply will be related to a wide variety of energy resources, especially including renewable ones. Besides, energy production in a particular region should be related to its natural energy resources, as for instance solar and biomass. On other hand, gas turbines versatility, dynamic operation and reduced water consumption enable them to operate in an standard open cycle way by using traditional fuels or taking advantage of solar resources or biomass in regions with good insolation or biomass stocks. This is feasible because can work also in a closed cycle or externally fired (EFGT) [1]. The aim of this work is to present and validate a thermodynamic model for an EFGT power plant hybridized with a central tower solar collector. This scheme would provide electric energy in a purely renewable way. Previous works have focused on the hybridization of standard natural gas turbines with a solar subsystem [2] or to evaluate the performance of EFGTs with several types of biomasses [3]. But to our knowledge, there are not many neither experimental nor computational works on biomass fueled EFGTs hybridized with a central tower solar field.

THERMODYNAMIC CYCLE.

The cycle starts when air at ambient conditions (pressure P1 and temperature T1) passes through Nc non adiabatic compressors equipped with (Nc-1) intercoolers to finally reach pressure P2 and temperature T2. The intercoolers are situated between each pair of compressors to decrease the air exit temperature to T1 before entering the next compressor. After this process the air is pre-heated in a solar tower before reaching the entrance of a high temperature heat exchanger (HTHE). In the HTHE the air is heated by combustion gases coming from a combustion chamber to temperature T3 which must be settled taking into account constructive and metallurgical limits. In order to reach this temperature the fuel mass flow entering the combustion chamber is calculated. After heated, the air is expanded through Nt turbines to pressure P4 and temperature T4. The expanded air now enters the combustion chamber where it is burned along with the biomass and after exchanging power in the HTHE it is released to the ambient. A scheme of the plant and a T-S diagram of the process are shown in figure 1 (a) and (b) respectively.

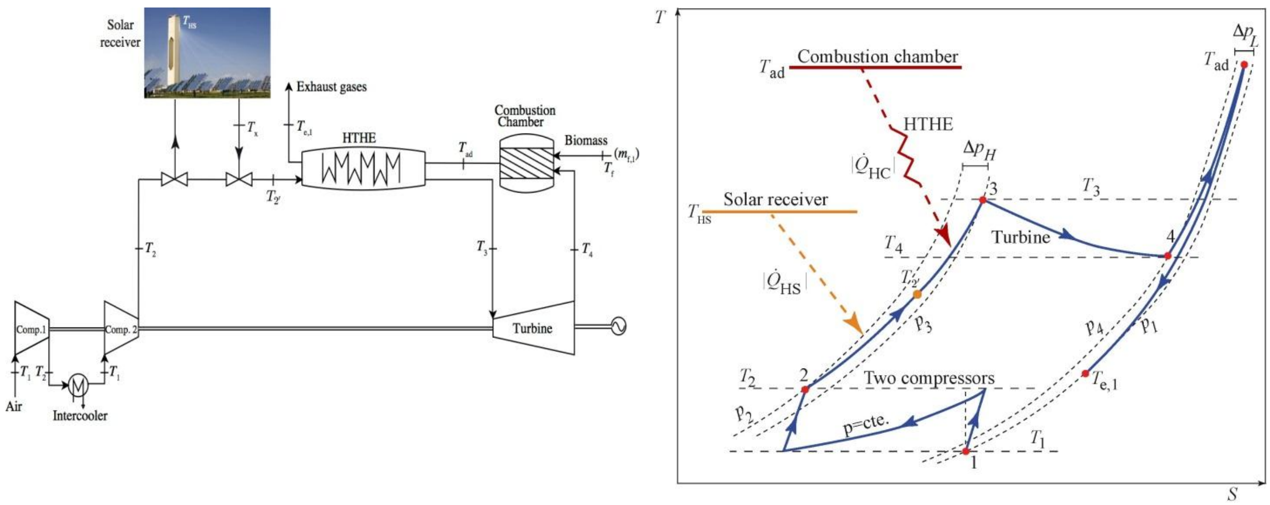

(a) Scheme (b) T-S diagram

FIGURE 1. Plant scheme (a) and T-S diagram of the thermodynamic cycle experienced by the working fluid.

PLANT MODEL.

As the actual receiver placed in Solugas allows a 5.6 kg/s air mass flow a bypass was implemented. The air exiting the compressor (at temperature T_2) is divided before the receiver and mixed afterwards before the HTHE entrance. As shown in figure 1(a), the air exiting the receiver reaches temperature T_x while the temperature at the HTHE entrance is $T_{2\prime}$. The plant model is the one presented in [4], the main equations implemented are presented below

$$T_2 = T_1 \left[1 + \frac{a_c - 1}{\varepsilon_c}\right] \tag{1}$$

where

$$a_c = r_c^{\frac{\gamma_{12}-1}{\gamma_{12}}} \tag{2}$$

and

$$r_c = \left(\frac{p_2}{p_1}\right)^{\frac{1}{N_c}} \tag{3}$$

γ_{12} represents the mean adiabatic coefficient in the expansion and ε_c the isentropic efficiency of each compressor. For the pressure loss the following adjustable parameter was introduced

$$\rho = \left(\frac{p - \Delta p}{p}\right)^{\frac{\gamma - 1}{\gamma}} \tag{4}$$

The turbine exhaust temperature is calculated using (5) while a_t is found analogous to eq. (2) and ε_t is the turbine isentropic efficiency.

$$T_4 = T_3 \left[1 - \varepsilon_t \left(1 - \frac{1}{a_t}\right)\right] \tag{5}$$

For a more detailed insight of the model refer to [4].

SOLAR POWER TOWER MODEL

The solar receiver considered in the model is the one placed in the SOLUGAS tower developed by ABENGOA in 2009 situated in Spain. The central tower (of 77m height) is pointed by a maximum number of 69 heliostats each one of 121.3m^2. The receiver consists of 10 panels each one formed by 17 absorber tubes, with an 19.6mm inlet diameter, 22.4mm outer diameter and a total length of 5m. A picture of the SOLUGAS tower and receiver is presented in figure 2.

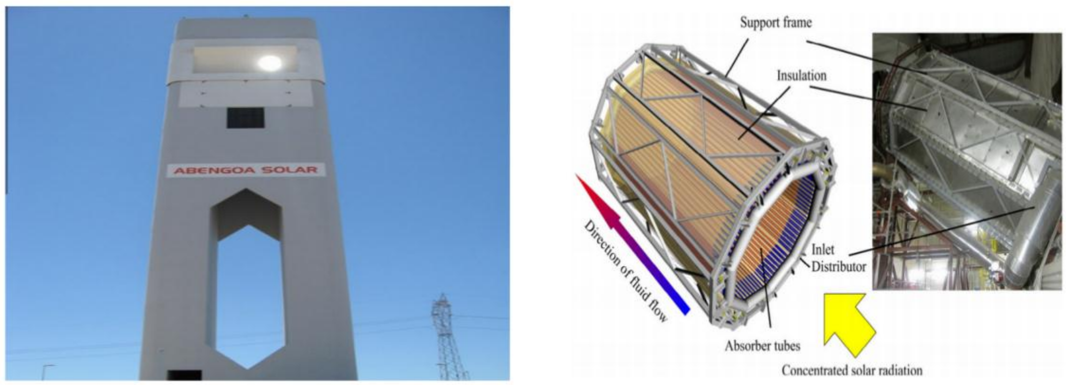

(a) Tower (b) Receiver

FIGURE 2. Pictures of the central tower (a) and the receiver (b) of the Solugas project. Reprinted from [7] with permission from Elsevier.

Two models where implemented as it is detailed in the following subsections.

Model 1

This model is presented in [5] and consists on the following balance.

$$Q_{air} = \eta_{sol} G A_{col} - \varepsilon_{eff} \sigma A_{rec} \left({T_{rec}}^4 - {T_{amb}}^4 \right) - U_L A_{rec} (T_{rec} - T_{amb}) \tag{6}$$

where Q_{air} is the heat gained by the air in the receiver, η_{sol} the fraction of the incident radiation that reaches the receiver, G the direct normal irradiance, A_{col} the aperture area of the collector, A_{rec} the absorber area of the receivers, ε_{eff} the effective emissivity, σ the Stefan-Boltzmann constant, T_{amb} the ambient temperature (K), T_{rec} the working temperature of the solar receiver and U_L the convective losses of the solar collector. η_{sol} was estimated using data presented in [6] where an operating point was presented, this means DNI, number of aligned heliostats and the solar input power into the aperture of the receiver were specified. The tubes effective emissivity was calculated by considering an emissivity value of 0.9 and affecting it by the view factor between the receptor and aperture surfaces. As there is no experimental data regarding the convection coefficient, a least squares method was applied in order to find the coefficient which better fix the experimental information presented in [7].
With the convective losses of the solar collector (U_L) obtained from this method is possible find the outlet receiver temperature. The final values obtained where U_L= 17.142$\frac{w}{m^2k}$, ε_{eff}= 0.11167, η_{sol} = 0.503 and the error committed with the least squares method varies between 2% and 11%.

Model 2

The other model considers a cylindrical cavity formed by 3 surfaces (surface 1 represents the cavity aperture, surface 2 the absorber tubes area and surface 3 the back wall) which receives energy at solar spectrum and emits in

infrared frequencies. Convection losses are also taken into account. A radiosity method is implemented to solve the cavity, at both, the solar and infrared spectrum as presented in [8]. The heat gained by the surfaces at the solar spectrum (Q_2 and Q_3) is then released at infrared spectrum as shown below
At solar spectrum:

$$J_{1s} = \eta_s \sigma A_{col} \tag{7}$$

$$A_2 J_{2s} = \rho_2 (A_1 J_{1s} F_{12} + A_2 J_{2s} F_{22} + A_3 J_{3s} F_{32}) \tag{8}$$

$$A_3 J_{3s} = \rho_3 (A_1 J_{1s} F_{13} + A_3 J_{2s} F_{32}) \tag{9}$$

The heat gained by the surface 2 and 3 can be expressed in the following way.

$$Q_2 = (J_{3s} - J_{2s}) F_{32} A_3 + (J_{1s} - J_{2s}) F_{12} A_1 \tag{10}$$

$$Q_3 = (J_{1s} - J_{3s}) F_{13} A_1 + (J_{2s} - J_{3s}) F_{32} A_3 \tag{11}$$

At infrared spectrum:

$$Q_3 = (J_3 - J_2) F_{32} A_3 + \left(J_3 - \sigma {T_{amb}}^4\right) F_{13} A_1 \tag{12}$$

$$(J_3 - J_2) F_{32} A_3 + \left(\sigma {T_{amb}}^4 - J_2\right) F_{12} A_1 = \left(J_2 - \sigma {T_{rec}}^4\right) \frac{\varepsilon_2 A_2}{1 - \varepsilon_2} \tag{13}$$

$$\left(J_2 - \sigma {T_{rec}}^4\right) \frac{\varepsilon_2 A_2}{1 - \varepsilon_2} + Q_2 = Q_{air} + h(T_{rec} - T_{amb}) A_2 \tag{14}$$

Where $Q_{air} = ef\ \dot{m}\ C_p (T_{rec} - T_{air,in})$. The HTHE efficiency was obtained from eq ()

$$ef = \frac{T_{air,out} - T_{air,in}}{T_{rec} - T_{air,in}} \tag{15}$$

The outlet receiver temperature predicted by both models is plotted against 15 experimental points presented in [7]. The result is shown below

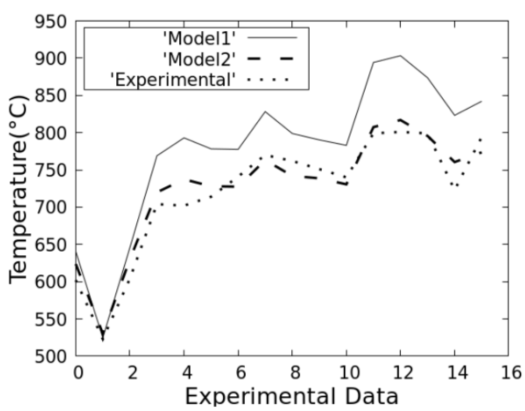

FIGURE 3. Temperature predictions.

TURBINE

Model

The model is presented and validated in [4] and consists in solving the combustion and heat transfer problem. On one hand, since the heat gained by the air in the HTHE in order to reach the fixed temperature T3 is determined, so the adiabatic temperature Tad should be reached at the exit of the combustion chamber. The way of controlling this temperature is by varying the combustion equivalence ratio. The equations implemented are shown below:

$$T_{ad} = \frac{T_{turbine,out} - T_{tubrine,in}}{\varepsilon} + T_{turbine,in} \tag{16}$$

$$h_{fuel} = Cp_{fuel}\left(T_{fuel} - T_{ref}\right) + LHV_{fuel} - f\left[hfg_{H_2O} - C_{p,H_2O}\left(T_f - T_{ref}\right)\right] \tag{17}$$

$$h_g(T) = x_{co_2}h_{co_2}(T) + x_{H_2O}h_{H_2O}(T) + x_{o_2}h_{o_2}(T) + x_{N_2}h_{N_2}(T) \tag{18}$$

$$\acute{m}_{fuel}h_{fuel}\left(T_{fuel}\right) + \acute{m}_{air}h_{air}(T_{air}) = \acute{m}_{gases}h_{gases}(T_{ad}) \tag{19}$$

The following expressions were used for determining Tad in equation (16).

$$\varepsilon = \frac{1-e^{-NTU(1-c_r)}}{1-c_r e^{-NTU(1-c_r)}} \tag{20}$$

$$NTU = \frac{k}{c_{min}\left(\acute{m}_{air}{}^{-0.8} + \acute{m}_{gases}{}^{-0.6}\right)} \tag{21}$$

where k is a constant that depends on the heat exchanger geometry and construction material (see [4] for details).

Parameter

Mercury 50 Gas turbine was considered in the model. The main turbines parameters are shown in table 1 while the pressure loss in the installation is taken as an input parameter. The compressor and turbine isentropic efficiencies where obtained considering data presented in [7] where ambient temperature, the compressor discharge gauge pressure, the turbine inlet temperature and the compressor discharge temperature where specified. For the determination of both efficiencies a 16.7 $\frac{kg}{s}$ was employed.

TABLE 1. Turbine parameters.

Item	Quantity
Power ISO conditions	4600kW
Pressure ratio	10
Mass flow	16.7(kg/s)
Compressor efficiency	0.843
Turbine efficiency	0.822

RESULTS

A one year simulation situated in Uruguay was run using a biomass with the following composition C = 49.3%, H = 6%, O = 44.4%, N < 0.01%, Ash = 0.3% with a low heating value of 18681 kJ/kg, considering the irradiation and ambient temperature data from LES (Laboratorio de Energía Solar). The power output, fuel mass flow, total and economic efficiency results are presented. Total efficiency is calculated as the obtained output power divided over the power entering the plant, the enthalpies are referenced at 298 K.

$$\eta_{total} = \frac{Power}{\dot{Q}_s + \dot{m}_f h_f + \dot{m}_a h_a} \tag{22}$$

While the economic efficiency is expressed as

$$\eta_{econ} = \frac{Power}{\dot{m}_f Qpi} \tag{23}$$

In figure 4 it can be noted that the power output increases in winter. This can be explained since the power obtained from the turbine remains constant as the inlet temperature is a fixed parameter while the power required by the compressor decreases as the ambient temperature is lower.

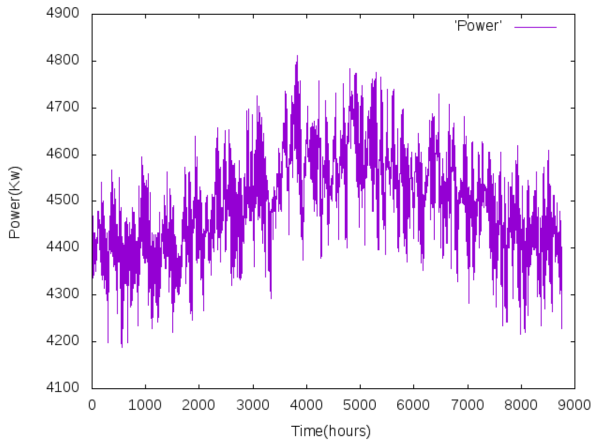

FIGURE 4. Yearly evolution of the output power.

Due to the arguments expressed above an increase in fuel consumption during winter is expected, this effect can be observed in figure 5.

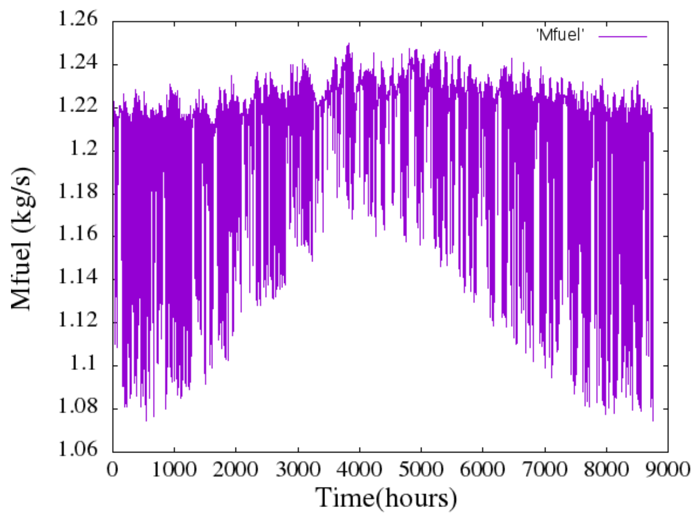

FIGURE 5. Yearly evolution of fuel consumption.

As it is shown in figure 6 (a) the total efficiency is around 0.20 which is lower than other hybrids plants presented, for example in [7] a total efficiency of 0.27 is predicted. This difference can be explained since the model considers a externally fired gas turbine, this leads to higher gases temperature which means higher spillage in the exhaust gases.

Finally economic efficiency is shown in figure 6 (b), reaching values of around 0.23-0.24 during summer.

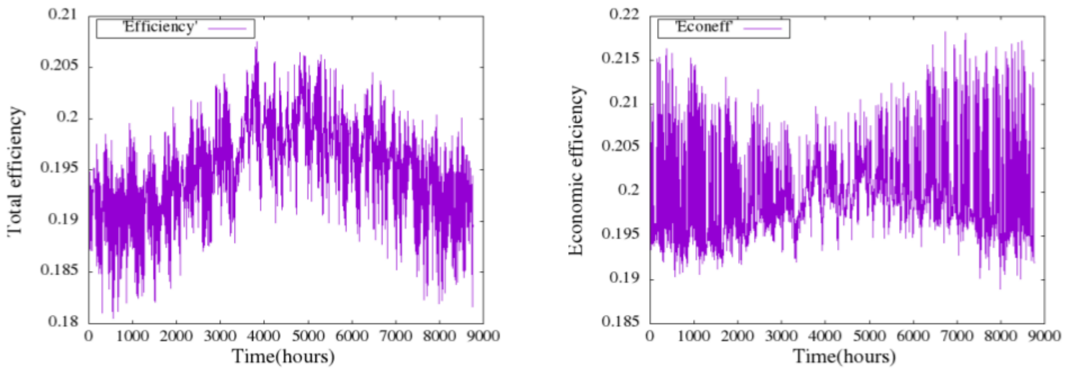

(a) Total efficiency (b) Economic efficiency

FIGURE 6. Evolution of the overall plant efficiency (a) and the fuel conversion efficiency (b) as functions of time during a typical year.

In figure 7 typical summer and winter days temperature evolution is shown. It can be noted that T_4 remains constant (as expected by setting T_3), while small variations of ambient temperature can be appreciated. The main difference lies in the collector outlet temperature, that reaches temperatures of about 1100 K in summer and 800 K in winter.

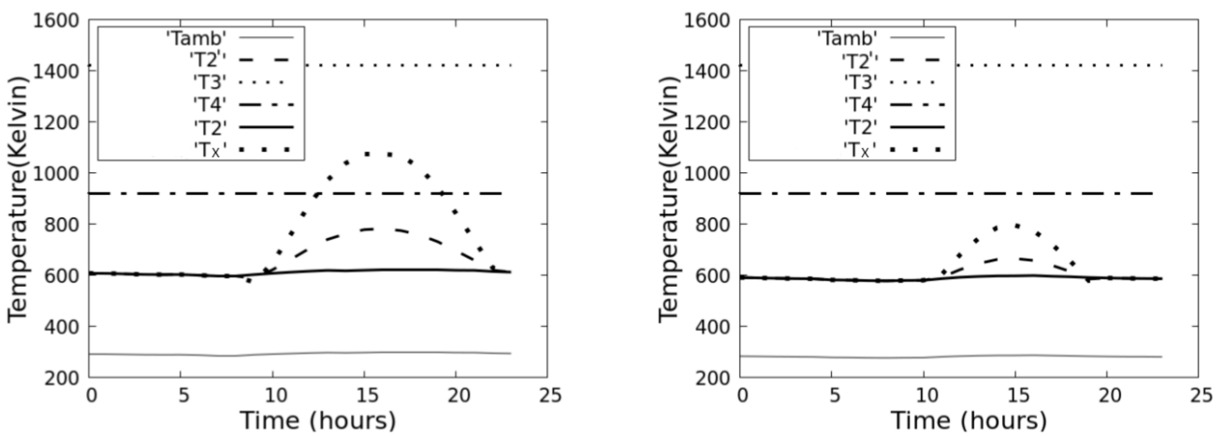

(a) Summer (b) Winter

FIGURE 7. Evolution of main temperatures in the thermodynamic cycle for typical summer (a) and winter (b) days.

In order to obtain global results a comparison between the hybrid and non-hybrid plant for a year simulation is presented. It must be noted that the power obtained is the same since it only relies on the ambient temperature, compressor isentropic efficiency, turbine isentropic efficiency and the fixed temperature T3.

The total energy obtained is 141.78 TJ with a predicted biomass consumption of $3.8\text{x}10^7$ kg for the hybrid plant what leads to a 19.97% economic efficiency. On the other hand, without considering the solar tower the biomass mass predicted ascends to $3.86\text{x}10^7$ kg, which leads to an economic efficiency value of 19.66%.

CONCLUSIONS.

A thermodynamic model for a hybrid thermo-solar externally fired gas turbine power plant fueled with biomass was successfully developed. Power output and total and economic efficiencies for a plant situated in Uruguay were obtained from a year simulation. The most important results were:

- The power obtained from the plant varies between 4800(kW) and 4200 (kW), reaching the maximum during winter due to a decrease in the compressors power consumption.
- As expected the fuel required during winter results higher than in summer. While in summer it varies from 1.08(kg/s)-1.22 (kg/s) in winter the range is 1.17(kg/s)-1.24(kg/s).
- A 2% rise can be observed in the instant economic efficiency at good radiation conditions but also a 1% increment can be appreciated at no so favorable conditions.
- Due to the low fuel saving it can be noted that the solar field and tower cavity seem to be undersized. This can also be appreciated considering that at the best radiation conditions the solar energy represents only a 25% of the total energy needed.
- In Solugas plant, a maximum temperature of 650 ºC is allowed at the combustion chamber entrance. In this work, since the combustion is external, this restriction could be removed. However, some limitation to this temperature could exist due to technological issues in the HTHE.
- Finally an increase in the plant efficiency could be reached if a recuperator or bottoming cycle is considered, using the available energy of the combustion gases exiting the HTHE or the air exiting the turbine.

FUTURE RESEARCH

- The design of an appropriate solar field and tower cavity, leading to greater temperatures at the tower outlet and an increment in the mass flow allowed at this component must be considered.

- In addition, a recuperator or bottoming cycle implementation should be evaluated in order to increase the total plant efficiency.

- Finally other configurations, such as placing the solar tower after the HTHE, can be also evaluated. This new configuration would increase the plant efficiency by decreasing the released gases temperature and thus, the spillage.

ACKNOWLEDGMENTS

A.M. and A.C.H. acknowledge financial support from University of Salamanca.

REFERENCES

1. M. Kautz and U. Hansen. The externally fired gas turbine (EFGT-cycle) for decentralized use of biomass, Appl. Ener., 84, 795-805 (2007).
2. M. Jamel, A. Abd Rahman and A. Shamsuddin. Advances in the integration of solar thermal energy with conventional and non-conventional power plants, Renew. Sust. Ener Rev., 20, 71-81 (2013).
3. K. Al-Attab and Z. Zainal. Externally fired gas turbine technology, Appl. Ener., 138, 474-487 (2015).
4. A. Durante; G. Pena-Vergara; P.L. Curto-Risso; A. Medina; A. Calvo Hernández. Thermodynamic simulation of a multi-step externally fired gas turbine powered by biomass, Ener. Conv. Manage., 140 (15) 182-191 (2017).
5. M.J. Santos, R.P. Merchán, A. Medina, A. Calvo Hernández. Seasonal thermodynamic prediction of the performance of a hybrid solar gas-turbine power plant,. Ener. Conv. Manage., 115, 89-102 (2016).
6. M. Ebert, D.Benitez, M. Röger, R. Korzynietz, J.A. Brioso. Efficiency determination of tubular solar receivers in central receiver systems. Sol. Ener., 139 (1), 179-189 (2016).
7. R. Korzynietz, J.A. Brioso, A. del Río, M. Quero, M. Gallas, R. Uhlig, M. Ebert, R. Buck, D. Teraji. Solugas – Comprehensive analysis of the solar hybrid Brayton plant, Sol. Ener., 135, 578-589 (2016).
8. T. Bergman, A. Lavine, F.Incropera, D. Dewitt, “Radiation Exchange Between Surfaces” in Fundamentals of heat and mass transfer, Wiley, 2012.